



Formation control and collision avoidance for multi-agent systems based on position estimation

Yuanqing Xia*, Xitai Na, Zhongqi Sun, Jing Chen

School of Automation, Beijing Institute of Technology, Beijing 100081, PR China

ARTICLE INFO

Article history:

Received 13 March 2015

Received in revised form

11 November 2015

Accepted 15 December 2015

Keywords:

Formation control

Second-order systems

Optimal control

Collision avoidance

ABSTRACT

In this paper, formation control strategies based on position estimation for double-integrator systems are investigated. Firstly, an optimal control formation control strategy is derived based on the estimator. It is proven that the control inputs are able to drive the agents to the predefined formation and the controller is optimal even based on the estimation law if the estimator has converged to stable. Secondly, a consensus law based on the estimator is presented, which enables the agents converge to the formation in a cooperative manner. The stability can be guaranteed by proper parameters. Thirdly, extra control input for inter collision avoidance is added into the derived consensus control strategy, and efficacy analysis are provided in detail. Finally, the effectiveness of the strategies proposed are shown by simulation and experiment results.

© 2015 ISA. Published by Elsevier Ltd. All rights reserved.

1. Introduction

With the widely use of multi-agent, scholars are also growing their interest in agent's algorithm study. The research of multi-agent mainly focus on agents' formation control, and obstacle avoidance [1,3]. The cooperative control of multi-agent systems can be categorized as single-integrator system [4], double-integrator system [5], high-order system [6] and some more complex dynamics such as distributed-order fractional damping system [7] and nonholonomic robotic system [8,9].

The essence of formation control is the strict geometry coalescence control [1,4]. The purpose of formation control is to realize specified configuration or to reach to desired target point by adjusting individual's behavior. Formation control has many research methods now, we can be roughly divided into three categories: leader–follower, virtual structure and behavior based method. The leader–follower approach plus the Lyapunov and sliding mode methods are used in [11] and [12] to design cooperative controllers for a group of underactuated vessels. A combination of line-of-sight path-following and nonlinear synchronization strategies is studied in [13] to make a group of underactuated vessels asymptotically follow a given straight-line path with a given forward speed profile. Virtual structure is a widely used formation control method [14], whereas, it is only suitable for formation control with less individuals. In recent years, Beard et al. [15] have done a lot of fruitful work by using

distributed frame to realize virtual structure formation. Actually, the formation control based on behavior method is not often used, yet the typical literature include [16] and [17].

As nodes move to achieve a desired configuration they must avoid obstacles and remain connected. Navigation functions are originally developed in the seminal work in [18] to enable a single point-mass agent to move in an environment with spherical obstacles. The navigation function developed in [18] is designed to be a real-valued function that is designed so that the negated gradient field does not have a local minima and the agents' performance converges to a desired destination. Results such as [19] and [20] are motivated by the need to prevent the graph partitioning.

In most of these applications, strong ability of communication is needed by each individuals, in other words, the absolute position of each agent is required to carry out the following work such as formation control, consensus control and rendezvous control. But in order to get the exact location, it has to build a localization platform, which costs highly. Even if the localization platform is ready, in many cases we also cannot obtain the absolute position of agents, for instance the transmission fault, the limitations of the hardware and the factor of the energy costs make it difficult to get the absolute position. However, the real-time relative position of the multi-agents can be easily measured by using infrared detection or bluetooth devices. The velocity of each individual can also be obtained from calculating the distance of adjacent two detection times by the photosensitive elements.

The works presented in this paper are based on our precious work [2] and the estimator proposed in [24]. However, the

* Corresponding author.

E-mail address: xia_yuanqing@bit.edu.cn (Y. Xia).

controllers designed in this paper are quite different from [24], in which the estimation law is presented based on single-integrator system, and use unicycle systems to test its efficacy. The linear velocity of the unicycle is designed as a PD-like feedback law, which in fact is assumed to be a single integrator system, while the angular velocity is designed as a periodic time-varying cosinoidal function and is independent of states information. While in this paper, we expend its application into double-integrator systems. The main contribution can be summarized as follows: (a) an optimal control law based on the maximum principle is designed based on the estimator for the second order systems. It also has been proven that the control inputs are able to drive the agents to the predefined formation, and is optimal even based on the estimation law if the estimator converges to stable; (b) the consensus law based on the estimator is presented, which enables the agents converge to the formation in a cooperative manner. The stability can be guaranteed by proper parameters; (c) we further studied the inter collision avoidance scene based on the estimator and the consensus law presented, and provided the efficacy analysis in detail.

The structure of this paper is organized as follows. In Section 2, some basic knowledge of graph theories and some necessary preliminary results for formation background are presented. Section 3 states the model and problems we studied in this paper. Section 4 proposes an derived formation control strategy for the agents to realize cost limited while converging to the desired position puts forward the collision avoidance method used in this paper. Section 5 shows the results of the proposed control strategy to verify the proposed strategy and result of adding the extra control input which can realize obstacle avoidance effectively. In Section 6, we carried out experiments with the proposed algorithm. Finally, concluding remarks are given in Section 7.

2. Preliminaries

In this section, we introduce several notations in graph theory and list some useful notations for later reference.

A directed graph \mathcal{G} consists of a finite set of vertex $\mathcal{V}(\mathcal{G}) = \{v_1, v_2, \dots, v_n\}$ and an edge set $\mathcal{E} \subseteq \mathcal{V} \times \mathcal{V}$, where an edge is an ordered pair of vertices in $\mathcal{V}(\mathcal{G})$. If (v_i, v_j) is an edge of \mathcal{G} , v_i is defined as the parent vertex and v_j is defined as the child vertex. Let $\mathcal{G} = (\mathcal{V}, \mathcal{E}, A)$, where $A = [a_{ij}] \in \mathbb{R}^{|\mathcal{V}| \times |\mathcal{V}|}$ with non-negative elements, $|\mathcal{V}|$ denotes the cardinality of \mathcal{V} . The element a_{ij} of A is positive if $(v_i, v_j) \in \mathcal{E}$, which means there is a directed path from i to j , and it is zero otherwise. It is assumed that $(v_i, v_i) \notin \mathcal{E}$ for any $v_i \in \mathcal{V}$. The set of neighbors of $v_i \in \mathcal{V}$ is denoted by $\mathcal{N}_i = \{v_j \in \mathcal{V} : (v_i, v_j) \in \mathcal{E}\}$, called i 's communication set, which includes the agents with which agent i can communicate. A directed graph \mathcal{G} is said to have a spanning tree if there exists a vertex, called the root, such that it can be connected to all other vertices through paths. The node is called the root of the spanning tree. Here we concentrate on the directed graph which is often used in modeling communication topologies among agents. The degree d_i of the vertex i is defined by $d_i = \sum_{j \in \mathcal{N}_i} a_{ij}$. Let Δ be the $N \times N$ diagonal matrix of d_i . Then Δ is defined as the degree matrix of \mathcal{G} . The (combinatorial) Laplacian of \mathcal{G} is denoted by the positive semi-definite matrix $L = \Delta - A$. Here we have $L = [l_{ij}]$ of \mathcal{G} is

$$l_{ij} = \begin{cases} \sum_{k \in \mathcal{N}_i} a_{ik} & i = j \\ -a_{ij} & i \neq j. \end{cases}$$

The following result is recalled which will be used later.

Lemma 1 (Ren et al. [21]). Consider the linear system described by

$$\dot{x} = -Lx \quad (1)$$

where $x = (x_1, x_2, \dots, x_N) \in \mathbb{R}^N$ and L is the Laplacian matrix of a weighted directed graph \mathcal{G} . For (1), there exists a finite vector $x^\infty = (x_1^\infty, \dots, x_N^\infty) \in \mathbb{R}^N$ such that x exponentially converges to x^∞ if and only if \mathcal{G} has a spanning tree.

Lemma 2 (Ren and Beard [22]). Let

$$\rho_\pm = \frac{\gamma\mu - \alpha \pm \sqrt{(\gamma\lambda - \alpha)^2 + 4\mu}}{2} \quad (2)$$

where $\rho, \mu \in \mathbb{C}$. If $\alpha \geq 0$, $\text{Re}(\mu) < 0$, $\text{Im}(\mu) > 0$ and

$$\gamma > \Gamma(\mu) \quad (3)$$

where $\Gamma(\mu) = \frac{2}{\sqrt{|\mu| \cos \left[\tan^{-1} \frac{\text{Im}(\mu)}{-\text{Re}(\mu)} \right]}}$, then $\text{Re}(\rho) < 0$, where $\text{Re}(\cdot)$

and $\text{Im}(\cdot)$ represent, respectively, the real and imaginary parts of a number.

3. Problem formulation

3.1. System dynamics

Consider the second order linear system of the N -agents

$$\begin{cases} \dot{p}_i = v_i \\ \dot{v}_i = u_i \end{cases} \quad (4)$$

where $p_i \in \mathbb{R}^n$, $v_i \in \mathbb{R}^n$ and $u_i \in \mathbb{R}^n$ denote the position, velocity and control input of agent i , respectively. The overall system is rewritten as

$$\begin{cases} \dot{p} = v \\ \dot{v} = u \end{cases}$$

where $p = (p_1, \dots, p_N)$, $v = (v_1, \dots, v_N)$ and $u = (u_1, \dots, u_N)$. The interaction topology among the agents is modeled by a weighted directed graph $\mathcal{G} = (\mathcal{V}, \mathcal{E}, A)$, which is referred to as the interaction graph for the agents. As we have mentioned in Section 1, it is difficult to get agents' exact position p_i sometimes. To solve this problem, we first give the following assumptions:

- Agent i is able to sense the relative position of its neighbors, which is denoted as

$$p_{ij} = p_j^i = p_j - p_i, \quad \forall j \in \mathcal{N}_i \quad (5)$$

where p_j^i is the relative position of agent j to agent i , and cannot obtain the absolute position of the all agents.

- Each of the agent can measure its own absolute velocity v_i , $i = 1, \dots, N$ which is easy to get by calculating, and can obtain its neighbors' velocity information by communication.
- All the agents estimate their own positions denoted as \hat{p}_i , $i = 1, \dots, N$, and receive the values of the estimated position of their neighbors by communication.
- We assume agents are equipped with infrared and bluetooth function, which means the robot can explore the around environment, and it can take the corresponding collision avoidance measures once it explores other objects.
- Once agents $j(j \neq i)$ come into i 's communication region, they can communicate with each other (we use it only in obstacle avoidance).
- We assume there exists dynamic obstacles between agents themselves only, i.e. has no static obstacles in the environment.

For the agents modeled by (4), suppose that the interaction graph is given by $\mathcal{G} = (\mathcal{V}, \mathcal{E}, A)$ and the desired positions is $p_d = (p_{1d}, \dots, p_{Nd})$.

Lemma 3 (Ren and Beard [22]). For the system (4) with the following controller

$$u_i = - \sum_{j=1}^n a_{ij}(t) \left[(p_i - p_j) + \gamma(v_i - v_j) \right] \quad (6)$$

the system achieves consensus asymptotically if and only if Θ has exactly two zero eigenvalues and all other eigenvalues have negative real parts, where

$$\Theta = \begin{bmatrix} 0_{n \times n} & I_n \\ -L_n(t) & -\gamma L(t) \end{bmatrix}.$$

Specifically, $p_i(t) \rightarrow \sum_{i=1}^n \eta_i p_i(0) + t \sum_{i=1}^n \eta_i v_i(0)$ and $v_i(t) \rightarrow \sum_{i=1}^n \eta_i v_i(0)$ for large t , where $\eta = [\eta_1, \dots, \eta_n]^T \geq 0$, $\mathbf{1}_n^T \eta = 1$, and $L_n^T \eta = 0$.

3.2. Control objective

This paper studies the formation control problems for the agents as follows:

1. For each agent $i \in \mathcal{V}$, design an estimation law to achieve

$$\lim_{t \rightarrow \infty} \hat{p}_i(t) = p_i(t) + \tilde{p}_c^\infty \quad (7)$$

for a certain constant vector $\tilde{p}_c^\infty \in \mathbb{R}$ by using p_{ij} and \hat{p}_j for all $j \in \mathcal{N}_i$.

2. Given a group of desired position p_{id} , $i \in \mathcal{V}$, design an optimal control law based on the estimator designed such that all the agents can reach their desired position with a constant error, i.e.,

$$\begin{cases} \lim_{t \rightarrow \infty} p_i(t) = p_{id}(t) + \tilde{p}_c^\infty \\ \lim_{t \rightarrow \infty} v_i(t) = 0 \end{cases} \quad i \in \{1, \dots, N\} \quad (8)$$

where $\tilde{p}_c^\infty \in \mathbb{R}^n$ is constant vector, and the control energy cost is given by following quadratic performance index,

$$J = \frac{1}{2} \sum_{i=1}^N \left\{ \int_0^\infty [e_i(t)^T Q e_i(t) + u_i^T R u_i] dt \right\} \quad (9)$$

where Q and R are positive-definite matrices of appropriate dimensions, $e_i(t)$ is the output error $e_i(t) = p_{id} - \hat{p}_i$.

Remark 1. To find a control law u_i^* according to the maximum principle to minimize the performance index, absolute position and cost limited energy are required for the agent. The formation control problem of (4) is to track \hat{p}_i into the desired output p_{id} and consider the performance index (9) at the same time.

3. Design a consensus law based on the estimator, such that the agents converge to a consist view of the position and velocity, i.e.,

$$\begin{cases} \lim_{t \rightarrow \infty} p_i(t) = \lim_{t \rightarrow \infty} p_j(t) \\ \lim_{t \rightarrow \infty} v_i(t) = \lim_{t \rightarrow \infty} v_j(t) = \text{constant} \end{cases} \quad i, j \in \{1, \dots, N\} \quad (10)$$

4. Adding additional control input item based on the estimator into agents to realize collision avoidance while they converging to the desired position.

Remark 2. From the problem stated above, note the following points:

- The estimated position \hat{p}_i converges to $p_i + \tilde{p}_c^\infty$ rather than converges to p_i . More ever, v_i converges to a consist value of all the agents, which is determined by the initial velocity of each agent.
- p_i cannot converge to p_{id} exactly due to the error between \hat{p}_i and p_i .

- The data we can get are only p_{ij} , \hat{p}_i , \hat{p}_j and v_i by sensing, communication and calculation.

4. Design formation control law

4.1. Position estimator

A distributed position estimation law for the agents modeled by (4) can be designed as:

$$\dot{\hat{p}}_i = v_i + k_o \sum_{j \in \mathcal{N}_i} a_{ij}(\hat{p}_{ji} - p_{ji}) = v_i + k_o \sum_{j \in \mathcal{N}_i} a_{ij}[(\hat{p}_j - \hat{p}_i) - (p_j - p_i)] \quad (11)$$

where $k_o > 0$, \hat{p}_{ji} and p_{ji} are the estimated and real relative position between agent j and agent i , respectively. The second equal sign holds because $\hat{p}_{ji} = \hat{p}_j - \hat{p}_i$ and $p_{ji} = p_j - p_i$ which is mentioned above. (This equal sign is just for the stability analysis in the following article and the exact position p_j and p_i are not used in the simulation.)

The position estimation law (11) does not require the absolute position information but needs the velocity information v_i , relative position p_{ji} and additional information \hat{p}_j , which are obtained by calculating, sensing and communicating, respectively. Defining $\tilde{p}_i = p_i - \hat{p}_i$, and combining it with the first equation in (4) and (11), we obtain

$$\dot{\tilde{p}}_i = k_o \sum_{j \in \mathcal{N}_i} a_{ij}(\tilde{p}_j - \tilde{p}_i)$$

Rewrite the overall estimation error dynamic as

$$\dot{\tilde{p}} = -k_o(L_n \otimes I_m)\tilde{p} \quad (12)$$

where $\tilde{p} = (\tilde{p}_1, \dots, \tilde{p}_N)$, and \otimes denotes the Kronecker product of the matrices. The following result is useful in proving the convergence of \tilde{p} .

Lemma 4 (Oh [24]). For the estimation dynamics, there exists a finite vector $\tilde{p}^\infty = (\tilde{p}_c^\infty, \dots, \tilde{p}_c^\infty)$ such that \tilde{p} globally exponentially converges to $\tilde{p} - \tilde{p}^\infty$ if and only if \mathcal{G} has a spanning tree.

4.2. Control input based on position estimation and maximum principle

The differential equation (4) describes the linear time-invariant system and the second problem states that we need to find the optimal control $u^*(t)$, $t \in [t_0, \infty]$ to minimize the performance in (9), where $Q \geq 0$ and $R > 0$, both of them are constant symmetric matrices.

Rewriting (4) as the following format:

$$\begin{aligned} \dot{X}_i(t) &= A X_i(t) + B u_i(t) \quad X_i(t_0) = X_{i0} \\ Y_i(t) &= C X_i(t) \end{aligned} \quad (13)$$

X_i is a vector that $X_i = (x_{i1}, x_{i2}) = (p_i, v_i)$ and the performance index is

$$J_i = \frac{1}{2} \int_{t_0}^\infty \{ [p_{id}(t) - p_i(t)]^2 + u_i^2(t) \} dt \quad (14)$$

find the optimal control $u^*(t)$, to minimize J_i where $Q=1$, and $R=1$ in (9).

It is an infinite-time horizon quadratic problem and we will solve this problem according to the maximum principle.

From (4), we can obtain:

$$A = \begin{bmatrix} 0 & 1 \\ 0 & 0 \end{bmatrix}, \quad B = \begin{bmatrix} 0 \\ 1 \end{bmatrix}, \quad C = [1 \ 0],$$

and $Q = 1, R = 1$.

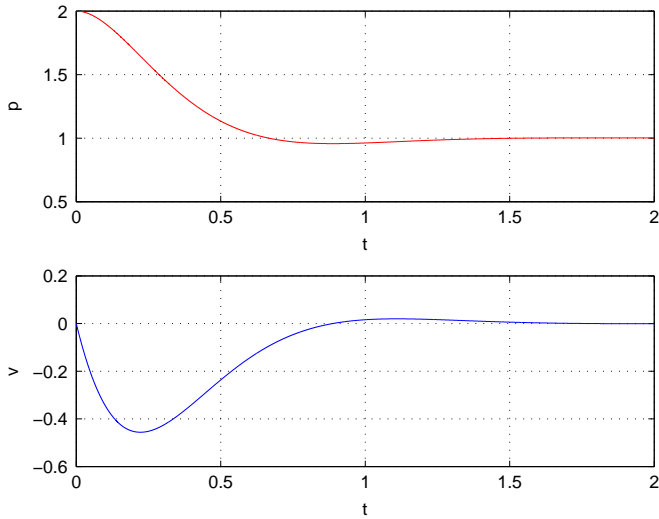


Fig. 1. The trajectory of (p_i, v_i) under the control input $u_i^*(t)$.

It is obviously that the system (A, B, C) is absolutely controllable and detectable, thus it exists the optimal control, which is

$$u_i^*(t) = -R^{-1}B^T P X_i(t) + R^{-1}B^T \eta(t) \quad (15)$$

where P and $\eta(t)$ are the solutions of the following algebraic equations:

$$\begin{aligned} PA + A^T P - PBR^{-1}B^T P + C^T Q C &= 0 \\ (PBR^{-1}B^T - A^T)\eta(t) - C^T Q y_r(t) &= 0 \end{aligned} \quad (16)$$

Denoting

$$P = \begin{bmatrix} p_{11} & p_{12} \\ p_{21} & p_{22} \end{bmatrix}$$

and substituting the value of A, B, C, P, Q into the first algebraic equation, as P is positive definite, we can obtain

$$p_{11} = \sqrt{2}, \quad p_{12} = p_{21} = 1, \quad p_{22} = \sqrt{2}$$

Calculating the same way as the first equation, we obtain

$$\begin{cases} \eta_2(t) = p_{id}(t) \\ \eta_1(t) = \sqrt{2}\eta_2(t) = \sqrt{2}p_{id}(t) \end{cases}$$

Thus,

$$u_i^*(t) = -x_{1i}(t) - \sqrt{2}x_{2i}(t) + p_{id}(t) = -p_i(t) - \sqrt{2}v_i(t) + p_{id}(t) \quad (17)$$

under the control input $u_i^*(t)$, (4) is stable apparently. The control input for the overall system is $u^*(t) = [u_1^*(t), \dots, u_N^*(t)]$.

Fig. 1 shows the trajectory of p_i and v_i under $u_i^*(t)$ when $p_{id} = 1, p_{i0} = 2, v_{i0} = 0$. The results show that $\lim_{t \rightarrow \infty} p_i(t) = p_{id}(t)$ and $\lim_{t \rightarrow \infty} v_i(t) = 0$ no matter where the original positions are. Based on different values of Q and R , we can also get the optimal control $u_i^*(t)$ using the same method.

In most cases, it is difficult to obtain the absolute position due to various reasons. But from (11), we can get the estimated position of agent i using only p_{ij} and \hat{p}_j where $j \in \mathcal{N}_i$. Combined the position estimator with optimal control input (17), since p_{id}, \hat{p}_i and v_i are available to agent i , a position control law for the agents can be designed as

$$u_i^*(t) = -\hat{p}_i(t) - \sqrt{2}v_i(t) + p_{id} \quad (18)$$

Theorem 1. For a team of N agents modeled as double integrator dynamics (4), suppose \mathcal{G} is the interaction graph and assume the graph \mathcal{G} contains a spanning tree. Given a desired formation described by $p_{id}, i = 1, 2, \dots, n$, there exists finite vectors $\tilde{p}^\infty = (\tilde{p}_1^\infty, \dots, \tilde{p}_n^\infty)$, such

that \hat{p} globally converges to $p + \tilde{p}^\infty$ and v_i converges to 0 under the controller (18) and the estimator (11). Furthermore, the controller (18) is optimal if the estimator has converged to stable.

Proof. Substituting (18) into (4), we obtain the following equation:

$$\begin{cases} \dot{p}_i = v_i \\ \dot{v}_i = -\hat{p}_i - \sqrt{2}v_i + p_{id} \end{cases} \quad (19)$$

as $\hat{p}_i = p_i - \tilde{p}_i$, then we have

$$\begin{bmatrix} \dot{p}_i \\ \dot{v}_i \end{bmatrix} = \begin{bmatrix} 0 & 1 \\ -1 & -\sqrt{2} \end{bmatrix} \begin{bmatrix} p_i \\ v_i \end{bmatrix} + \begin{bmatrix} 0 \\ p_{id} + \tilde{p}_i \end{bmatrix}$$

denoting p'_i and v'_i as:

$$\begin{cases} p'_i = p_i - (p_{id} + \tilde{p}_i) \\ v'_i = v_i \end{cases}$$

we obtain:

$$\begin{bmatrix} \dot{p}'_i \\ \dot{v}'_i \end{bmatrix} = \begin{bmatrix} 0 & 1 \\ -1 & -\sqrt{2} \end{bmatrix} \begin{bmatrix} p'_i \\ v'_i \end{bmatrix} + \begin{bmatrix} \dot{\tilde{p}}_i \\ 0 \end{bmatrix} \quad (20)$$

where $\dot{\tilde{p}} = -k_o(L_n \otimes I_m)\tilde{p}$, which implies that $\dot{\tilde{p}}_i$ and $\tilde{p} \rightarrow p_c^\infty$. It is obvious, from (20), that $p'_i \rightarrow 0$ and $v'_i \rightarrow 0$, which is equivalent to $p_i \rightarrow p_{id} + \tilde{p}_i$ and $v_i \rightarrow 0$.

Furthermore, if the estimator has converged to stable, the controller (18) can be rewritten as

$$u_i^*(t) = -p_i(t) - \sqrt{2}v_i(t) + p_{id}(t) + p_c^\infty$$

which is just the solution of (15) by setting the desired position as $p_{id}(t) + p_c^\infty$. This implies that the controller (18) is optimal to drive the agent from p_i to $p_{id}(t) + p_c^\infty$. This completes the proof. \square

Remark 3. The condition that the interaction graph contains a spanning tree is only used for ensuring the convergence of the estimator, and is not used for information exchange. The communication scene will be discussed in the next subsection.

4.3. Control input based on position estimation and consensus law

Based on the above assumption and the position estimator law, we propose the following state feedback controller for multi-agent system:

$$u_i = -\sum_{j=1}^n a_{ij} \left[(\hat{p}_i - p_{id} - (\hat{p}_j - p_{jd})) + \gamma(v_i - v_j) \right] \quad (21)$$

With (10), formation control is achieved or reached by the team of agents if, for all $i, j = 1, \dots, n$, $\|\hat{p}_i - p_{id}\| - \|\hat{p}_j - p_{jd}\| \rightarrow 0$ and $\|v_i - v_j\| \rightarrow 0$, as $t \rightarrow \infty$. As to achieve this effect, $\hat{p}_i \rightarrow p_{id}$ and $\hat{p}_j \rightarrow p_{jd}$ established.

Theorem 2. Let $\mu_i, i = 1, \dots, n$, denote as the i th eigenvalues of $-L_n$. Based on algorithm (21) and estimator (6), the multi-agent system can achieve the desired formation configuration if directed graph \mathcal{G} has a directed spanning tree and

$$\gamma > \bar{\gamma} \quad (22)$$

where $\bar{\gamma} \triangleq 0$ if all of the $n-1$ nonzero eigenvalues of $-L_n$ are negative and $\bar{\gamma} = \max_{\mu_i, i=1,2,\dots,n} \Gamma(\mu_i)$, otherwise. Therefore, for $t \rightarrow \infty$, there has:

$$\begin{aligned} p_i(t) &\rightarrow p_{id} + \tilde{p}_c^\infty + t \sum_{i=1}^n \eta_i v_i(0) \\ v_i(t) &\rightarrow \sum_{i=1}^n \eta_i v_i(0) \end{aligned} \quad (23)$$

where $\eta = [\eta_1, \dots, \eta_n]^T \geq 0$, $\mathbf{1}_n^T \eta = 1$, $L_n^T \eta = 1$, $p_d = (p_{1d}, p_{2d}, \dots, p_{nd})$, $\tilde{p}^\infty = (\tilde{p}_c^\infty, \tilde{p}_c^\infty, \dots, \tilde{p}_c^\infty)$ are constant.

Proof. Substitute the controller (21) in to the system (4), the system can be rewritten as

$$\begin{bmatrix} \dot{p} \\ \dot{v} \end{bmatrix} = \begin{bmatrix} 0_{n \times n} & I_n \\ -L_n & -\gamma L_n \end{bmatrix} \otimes I_m \begin{bmatrix} \dot{p} - p_d \\ v \end{bmatrix}$$

where $p = [p_1^T, p_2^T, \dots, p_n^T]^T$, $\hat{p} = [\hat{p}_1^T, \hat{p}_2^T, \dots, \hat{p}_n^T]^T$, and $p_d = [p_{1d}^T, p_{2d}^T, \dots, p_{nd}^T]^T$. Let $p_i - \hat{p}_i = \tilde{p}_i$ and

$$M = \begin{bmatrix} 0_{n \times n} & I_n \\ -L_n & -\gamma L_n \end{bmatrix},$$

we have

$$\begin{bmatrix} \dot{p} \\ \dot{v} \end{bmatrix} = (M \otimes I_m) \begin{bmatrix} p - \tilde{p} - p_d \\ v \end{bmatrix} = (M \otimes I_m) \begin{bmatrix} p - p_d \\ v \end{bmatrix} - \begin{bmatrix} 0 \\ (L_n \otimes I_m) \tilde{p} \end{bmatrix} \quad (24)$$

$$\dot{\tilde{p}} = -k_o(L_n \otimes I_m) \tilde{p} \quad (25)$$

From Lemma 4, we have $\tilde{p} \rightarrow [\tilde{p}_c^\infty, \tilde{p}_c^\infty, \dots, \tilde{p}_c^\infty]^T$. Combing with the proposition of Laplacian matrix L_n , one obtains $(L_n \otimes I_m) \tilde{p} \rightarrow 0$, as $t \rightarrow \infty$.

Next, we proof the matrix only have two zero eigenvalues and the all other eigenvalues have negative real parts. To find the eigenvalues of M , we can solve the equation $\det(\lambda I_{2n} - M) = 0$. Note that

$$\det(\lambda I_{2n} - M) = \det \left(\begin{bmatrix} \lambda I_n & -I_n \\ L_n & \lambda I_n + \gamma L_n \end{bmatrix} \right) = \det [\lambda^2 I_n + (1 + \gamma \lambda) L_n]$$

Also note that

$$\det(\lambda I_n + L_n) = \prod_{i=1}^n (\lambda - \mu_i) \quad (26)$$

where μ_i is the i th eigenvalue of $-L_n$. By comparing the above two equations, we see that

$$\det[\lambda^2 I_n + (1 + \gamma \lambda) L_n] = \prod_{i=1}^n [\lambda^2 - (1 + \gamma \lambda) \mu_i] \quad (27)$$

which implies that the roots of (26) can be obtained by solving $\lambda^2 = (1 + \gamma \lambda) \mu_i$. Therefore, it is straightforward to see that the eigenvalues of Θ are given by

$$\lambda_{i\pm} = \frac{\gamma \mu_i \pm \sqrt{\gamma^2 \mu_i^2 + 4 \mu_i}}{2} \quad (28)$$

where λ_{i+} and λ_{i-} are called the eigenvalues of M that are associated with μ_i . Eq. (28) implies that M only have two zero eigenvalues because that L_n only have one zero eigenvalue.

Since that the parameter satisfies (22), combining with the results given by Lemma 2, one can conclude that all the eigenvalues of M have negative real part except the two zero eigenvalues. Further, combining with the results given by Lemma 3 and the backstepping design technic, one obtains

$$\begin{aligned} p_i(t) &\rightarrow \sum_{i=1}^n \eta_i p_i(0) + p_{id} + t \sum_{i=1}^n \eta_i v_i(0) \\ v_i(t) &\rightarrow \sum_{i=1}^n \eta_i v_i(0) \end{aligned} \quad (29)$$

where $\sum_{i=1}^n \eta_i p_i(0) = \tilde{p}_c^\infty$. Since that p_d is constant and $\forall i = 1, 2, \dots, n$, \tilde{p}_c^∞ are all the same for each agent as time goes by, the final formation results can achieve as the desired formation configuration p_{id} . \square

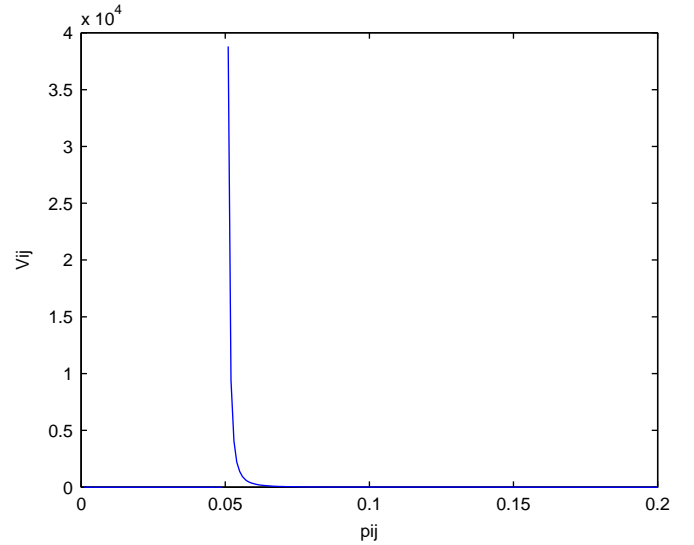


Fig. 2. The modified avoidance function where $r=0.05$ and $R=0.15$.

4.4. Control input based on position estimation and consensus law with collision avoidance

When implementing the formation control, complementary objectives derived from the systems' interaction constraints may also be considered. When converging to the desired position the allowed distance between agents which is a practical problem we need to consider. So collision avoidance constraints are necessary, we should add extra control terms during the formation control. The potential function based on the estimator is designed as follows:

$$V_{ij}(\hat{p}_i, \hat{p}_j) = \left(\min \left\{ 0, \frac{\|\hat{p}_i - \hat{p}_j\|^2 - R^2}{\|\hat{p}_i - \hat{p}_j\|^2 - r^2} \right\} \right)^2 \quad (30)$$

where R denotes the radius of the detection region and r denotes the avoidance region, i.e. the safety radius. If the distance between two agents is less than R , $V_{ij}(\hat{p}_i, \hat{p}_j)$ in (30) will be larger than zero and it will be effective in the extra control input. Also, Fig. 2 depicts the time evolution of the avoidance function $V_{ij}(\hat{p}_i, \hat{p}_j)$ which shows that as the distance between two agents tend to r , V_{ij} tends to ∞ . So we call r the safe distance.

The partial derivative of V_{ij} with respect to \hat{p}_i is given by

$$\frac{\partial V_{ij}}{\partial \hat{p}_i} = \begin{cases} \frac{4(R^2 - r^2)(\|\hat{p}_i - \hat{p}_j\|^2 - R^2)}{(\|\hat{p}_i - \hat{p}_j\|^2 - r^2)^3} (\hat{p}_i - \hat{p}_j)^T, & r \leq \|\hat{p}_i - \hat{p}_j\| \leq R \\ 0, & \|\hat{p}_i - \hat{p}_j\| \geq R \end{cases} \quad (31)$$

The consensus law with collision avoidance based on estimator is designed as follows:

$$u_i^a = - \sum_{j=1}^n a_{ij}[(\hat{p}_i - p_{id} - (\hat{p}_j - p_{jd})) + \gamma(v_i - v_j)] - \sum_{j=1}^n \frac{\partial V_{ij}(\hat{p}_i, \hat{p}_j)}{\partial \hat{p}_i} \quad (32)$$

Theorem 3. For the system (4), if the controller with consideration of collision avoidance is designed as (32), and the parameter γ is designed satisfying (22), then the system is able to build the formation defined as p_{id} , and the collision can be avoid.

Proof. Let $\xi_i = \hat{p}_i - p_{id}$, $i = 1, 2, \dots, n$. For system (4) with controller (21), a Lyapunov function candidate can be chosen as

$$V_1 = \frac{1}{2} \sum_{i=1}^n \sum_{j=1}^n [(\xi_i - \xi_j)^T (\xi_i - \xi_j) + (v_i - v_j)^T (v_i - v_j)] \quad (33)$$

Taking derivative of V_1 along the trajectories of the system, one obtains

$$\dot{V}_1 = \sum_{i=1}^n \sum_{j=1}^n [(\xi_i - \xi_j)^T (\dot{\xi}_i - \dot{\xi}_j) + (v_i - v_j)^T (u_i - u_j)] \quad (34)$$

It have been proven by [Theorem 2](#) that $(\xi_i - \xi_j) \rightarrow 0$ and $(v_i - v_j) \rightarrow 0$, for $i, j = 1, 2, \dots, n$, as $t \rightarrow \infty$. Consequently, $V_1 \rightarrow 0$ as $t \rightarrow \infty$, which implies $\dot{V}_1 \leq 0$, and the equals sign holds only when the system achieves consensus.

For system (4) with controller (32), we choose the Lyapunov function as follows:

$$V = \frac{1}{4} \sum_{i=1}^n \sum_{j=1}^n [(\xi_i - \xi_j)^T (\xi_i - \xi_j) + (v_i - v_j)^T (v_i - v_j)] + \sum_{i=1}^n \sum_{j=1}^n V_{ij}(\hat{p}_i, \hat{p}_j) \quad (35)$$

Taking derivative of V_1 along the trajectories of the system, for $i \neq j$, one can get

$$\begin{aligned} \dot{V} &= \frac{1}{2} \sum_{i=1}^n \sum_{j=1}^n [(\xi_i - \xi_j)^T (\dot{\xi}_i - \dot{\xi}_j) + (v_i - v_j)^T (u_i^a - u_j^a)] \\ &\quad + \sum_{i=1}^n \sum_{j=1}^n \left(\frac{\partial V_{ij}}{\partial \hat{p}_i} \dot{\hat{p}}_i + \frac{\partial V_{ij}}{\partial \hat{p}_j} \dot{\hat{p}}_j \right) = \frac{1}{2} \sum_{i=1}^n \sum_{j=1}^n [(\xi_i - \xi_j)^T (\dot{\xi}_i - \dot{\xi}_j) \\ &\quad + (v_i - v_j)^T (u_i - u_j)] - \frac{1}{2} \sum_{i=1}^n \sum_{j=1}^n \left[(v_i - v_j)^T \left(\sum_{k=1}^n \frac{\partial V_{ik}^T}{\partial \hat{p}_i} - \sum_{l=1}^n \frac{\partial V_{lj}^T}{\partial \hat{p}_j} \right) \right] \\ &\quad + \sum_{i=1}^n \sum_{j=1}^n \left(\frac{\partial V_{ij}}{\partial \hat{p}_i} \dot{\hat{p}}_i + \frac{\partial V_{ij}}{\partial \hat{p}_j} \dot{\hat{p}}_j \right) \end{aligned}$$

Due to the fact that $\dot{\hat{p}}_i = v_i$ if the estimator converges, and the fact that

$$\frac{\partial V_{ij}}{\partial \hat{p}_i} = -\frac{\partial V_{ij}}{\partial \hat{p}_j} = \frac{\partial V_{ji}}{\partial \hat{p}_i} = -\frac{\partial V_{ji}}{\partial \hat{p}_j} \quad (36)$$

it can be proven by expansion that the terms

$$\begin{aligned} &-\frac{1}{2} \sum_{i=1}^n \sum_{j=1}^n \left[(v_i - v_j)^T \left(\sum_{k=1}^n \frac{\partial V_{ik}^T}{\partial \hat{p}_i} - \sum_{l=1}^n \frac{\partial V_{lj}^T}{\partial \hat{p}_j} \right) \right] \\ &+ \sum_{i=1}^n \sum_{j=1}^n \left(\frac{\partial V_{ij}}{\partial \hat{p}_i} \dot{\hat{p}}_i + \frac{\partial V_{ij}}{\partial \hat{p}_j} \dot{\hat{p}}_j \right) = 0 \end{aligned} \quad (37)$$

Consequently,

$$\dot{V} = \frac{1}{2} \dot{V}_1 \leq 0 \quad (38)$$

which implies the system can achieve consensus and build the formation as same as p_{id} . On the other hand, for $i \neq j$, one has

$$\begin{aligned} \lim_{\|\hat{p}_i - \hat{p}_j\| \rightarrow r^+} V_{ij}(\hat{p}_i, \hat{p}_j) &= \infty \\ \lim_{\|\hat{p}_i - \hat{p}_j\| \rightarrow r^+} \frac{\partial V_{ij}(\hat{p}_i, \hat{p}_j)}{\partial \hat{p}_i} &= \infty \end{aligned} \quad (39)$$

We can conclude that the collision between agents can be avoided. \square

Remark 4. The potential function for collision avoidance designed is based on the estimator, which is different from others. The effectiveness of the collision avoidance function is, in fact, based on the assumption that the estimator has converged to stable. Certainly, we can use the relative position measured by sensors to avoid collision, and the assumption can be released. However, we found that the potential function designed based on estimator has better performance than based on measured relative position in

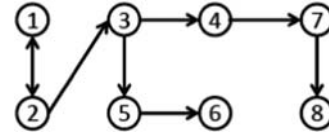


Fig. 3. The interaction graph.

experimental application. The reason may be that the estimator acted as a filter and thus is able to damp the sensor noises. But we did not discuss how the estimator damp the disturbance in this paper, and will consider it in our future work.

5. Simulation

5.1. Simulation results of control input based on position estimation and maximum principle

In this section, we present simulation results for eight second-order modeled agents. The interaction of communication graph for the eight agents is shown in [Fig. 3](#), in which the direction of an arrow indicates that of information flow between two corresponding agents.

[Fig. 4](#) shows the simulation results for the second-order modeled agents under the estimation law (11) and the control law (18) when $k_o = 1$. The trend of the control error $e = p_{id} - p_i$ and estimate error $\tilde{p}_i = p_i - \hat{p}_i$ are shown in [Fig. 5](#), where e_1 and e_2 are the average control error of all agents in x and y direction, respectively. In [Fig. 4](#), ‘*’ stands for the final position and ‘+’ stands for the desired position of each agent. We can note that they are not consistent, for the reason is the existence of \tilde{p}_c^∞ which we mentioned in [Lemma 4](#). We may also find the optimal value of k_o to minimize \tilde{p}_c using some intelligent method such as genetic algorithm.

[Fig. 5](#) illustrates that both the estimated error and control error are stabilized.

5.2. Simulation results of control input based on position estimation and consensus law

[Fig. 6](#) shows the trajectory of 8-agents based on consensus law (21), and in [Fig. 7](#), the estimated error and the control errors are depicted.

5.3. Simulation results of collision avoidance

Introducing additional collision avoidance control input on the second-order modeled agents under the estimation law (11) and the control law (21), [Figs. 8–11](#) show agents’ trajectory, the estimated error \tilde{p} and control error e of the system with three agents without and with avoidance control input.

[Fig. 8](#) depicts the trajectory of three agents with initial configuration $(-0.5, 0)$, $(-0.1, -0.4)$ and $(-0.2, -0.7)$ and destination $(-3, -2.9)$, $(-1, -0.7)$ and $(0, 1.2)$. In their way to desired position, they will collide in their trajectory. [Fig. 10](#) shows with extra control input, all of the three agents make their way round, so as to avoid collision. [Fig. 9](#) depicts the estimated error and control error converge to stable in the case of without adding avoidance. Also, [Fig. 11](#) shows the estimated error and control error ultimately tend to stable after a jitter in the coincide position. We can observe that the convergence rate shown in [Fig. 11](#) is slightly slowed down compared to that shown in [Fig. 9](#).

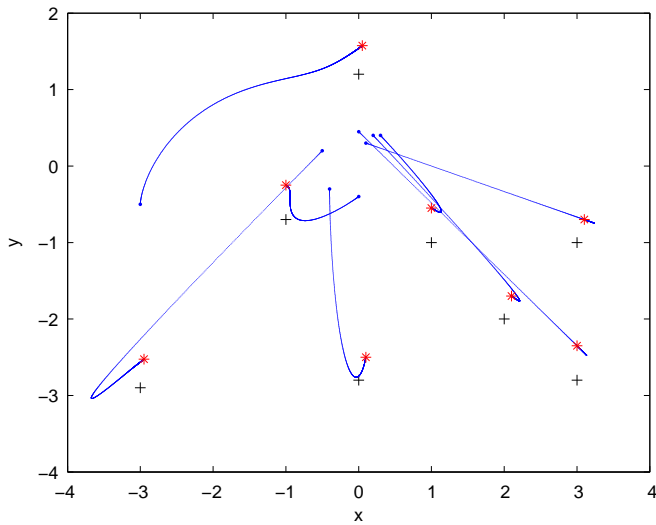


Fig. 4. The trajectory of 8-agents' position p .

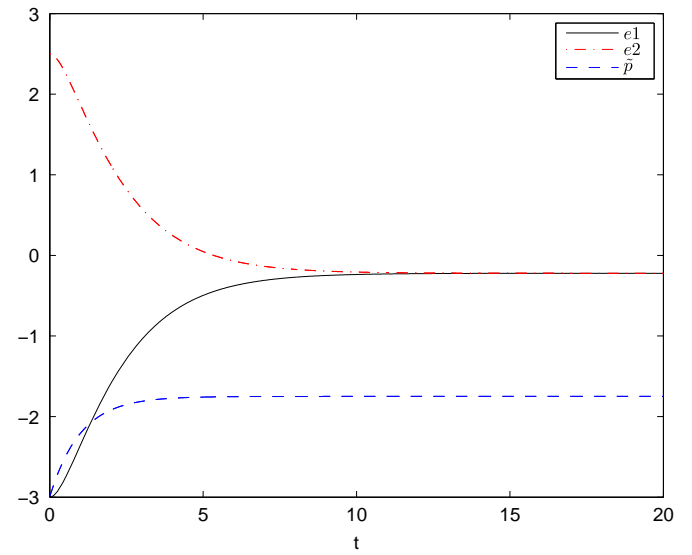


Fig. 7. The estimated error and control error of 8-agents based on consensus law.

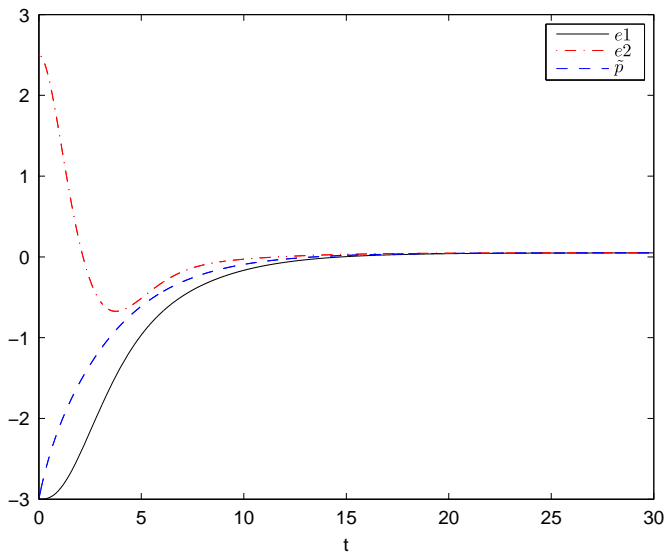


Fig. 5. The estimated error and control error.

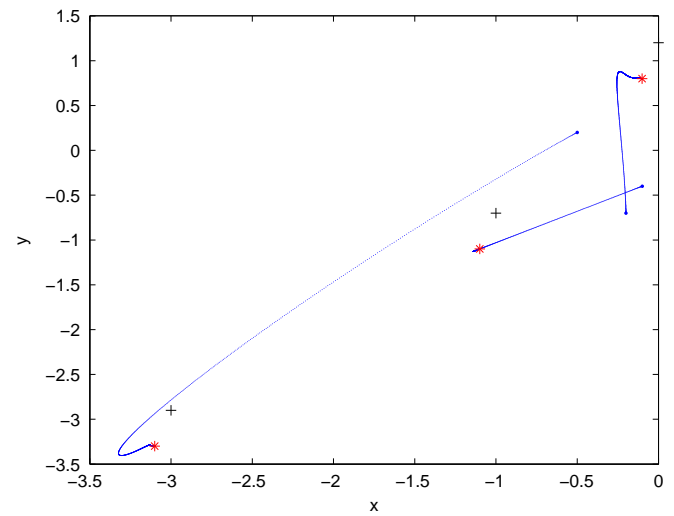


Fig. 8. Three agents' trajectory without added avoidance control input.

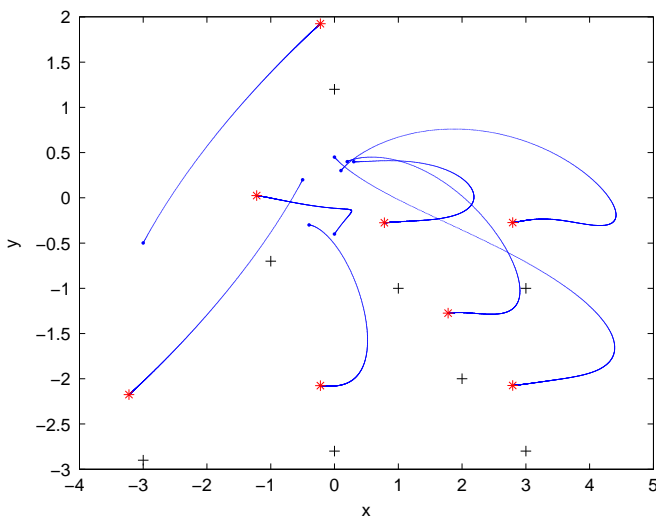


Fig. 6. The trajectory of 8-agents based on consensus law.

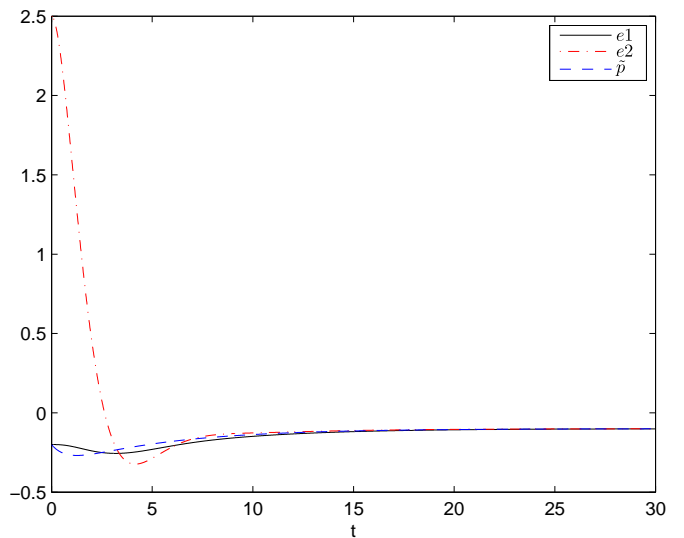


Fig. 9. The estimated error and control error without added avoidance control input.

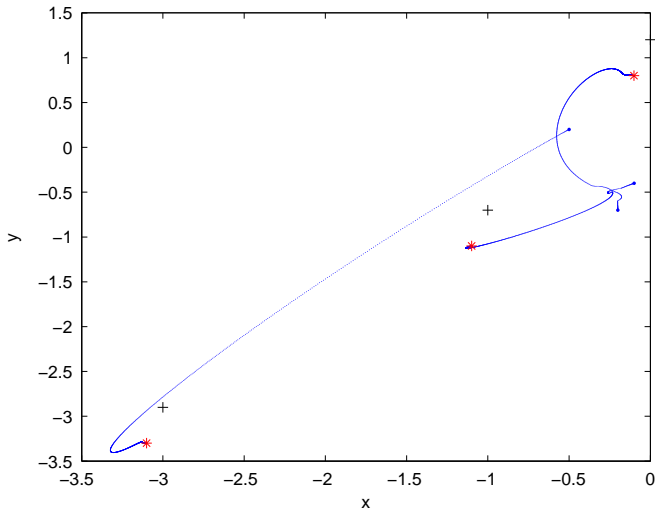


Fig. 10. Three agents' trajectory with added avoidance control input.

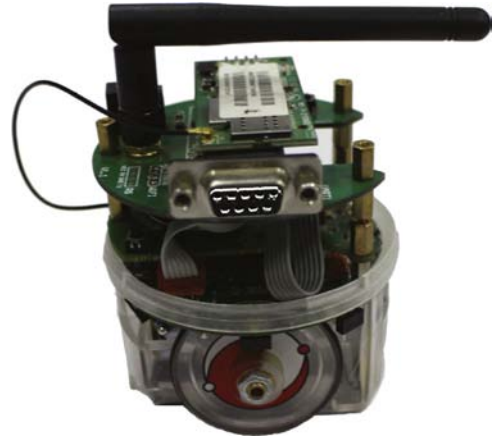


Fig. 12. The E-puck robot which we used to do the experiments.

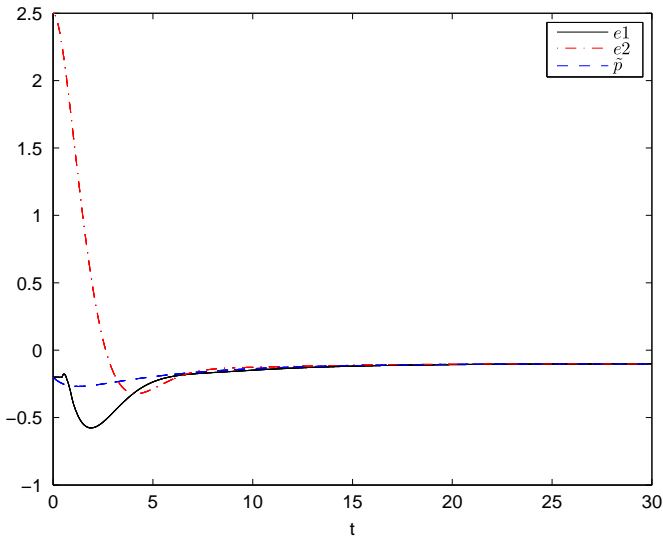


Fig. 11. The estimated error and control error with added avoidance control input.



Fig. 13. Experiments' platform.

6. Experiments

To demonstrate the effectiveness and the applicability of the proposed algorithm, we present some experimental results with a couple of E-puck robots. The E-puck is an educational robot and is very suitable for multi-agent cooperative experimentation. The robot is equipped with A3 axis accelerometer, three microphones, a speaker and a micro-camera. 8 IR proximity sensors are placed around the robot to detect the obstacles. Local processing is performed by a dsPIC microchip which has a dsp core allowing efficient data processing. Although blue-tooth is available for communication, we equip a Wi-Fi module to overcome the limits of blue-tooth in one-to-many communication. The modified robot is shown in Fig. 12.

The hardware architecture of the experimental platform is comprised of multi-agent system (E-pucks), overhead camera, and image processing station, as shown in Figs. 13 and 14. The overhead CCD camera is used to collect the multi-agent's image information, identify each agent, and determine the state information (including position and orientation) of the agents. Images from the camera are processed by the base station. The state information are transmitted through wireless Wi-Fi network.

Here we select three cars to experiment which colors are red, blue and yellow. E-puck receive their real-time position which are sent by PC through the wireless module. The frequency of PC emission data is 50 HZ, and the initial position of E-puck is arbitrary. The desired configuration of this article is triangle, and the position is $p_{1d} = (0, 0)$, $p_{2d} = (0.4, 0)$ and $p_{3d} = (0.2, 0.3)$. From PC's image acquisition software, we could see the final formation results in Fig. 14.

We set the data sampling period as 20 ms in our experiment. Figs. 15 and 16 show the trajectory of three agents without obstacle case. It can be observed that the agents are stabilized at $(0.801, 0.12)$, $(1.21, 0.45)$, and $(1.13, 0.14)$ from the initial configuration $(0.41, 0.54)$, $(0.7, 0.34)$, and $(0.63, 0.39)$, which verifies the validity of the strategy proposed.

Next, we put the agents at $(0.72, 0.68)$, $(1.25, 0.68)$, and $(0.83, 1.11)$ such that agent 1 and agent 2 may collide with each other. By implementing the strategy proposed, we can observe, from Figs. 17 and 18, that the collision avoidance function is activated between 300*20 ms and 600*20 ms, because they are too close to each other.



Fig. 14. The final results in the image acquisition interface.

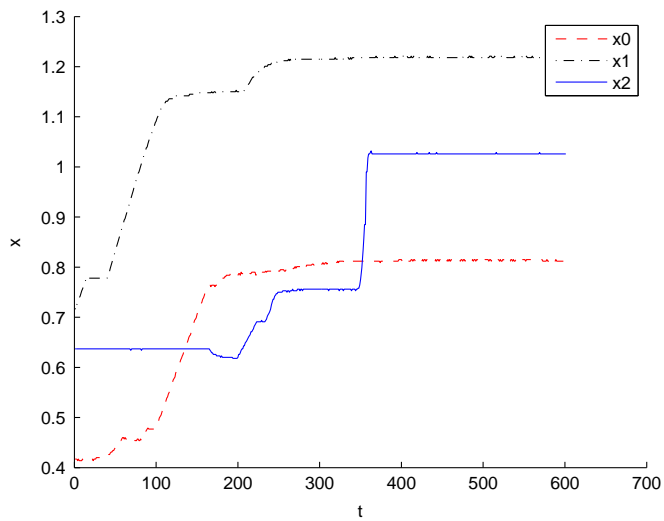


Fig. 15. The x coordinate of E-puck robots' position trajectory.

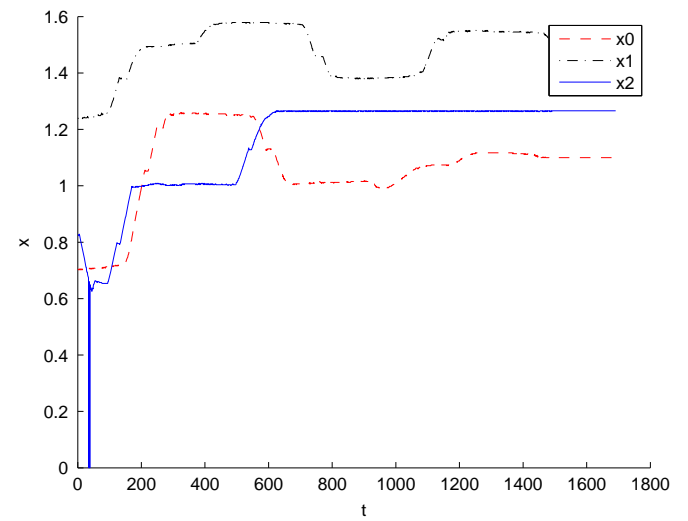


Fig. 17. The X coordinate of E-puck robots with collision avoidance.

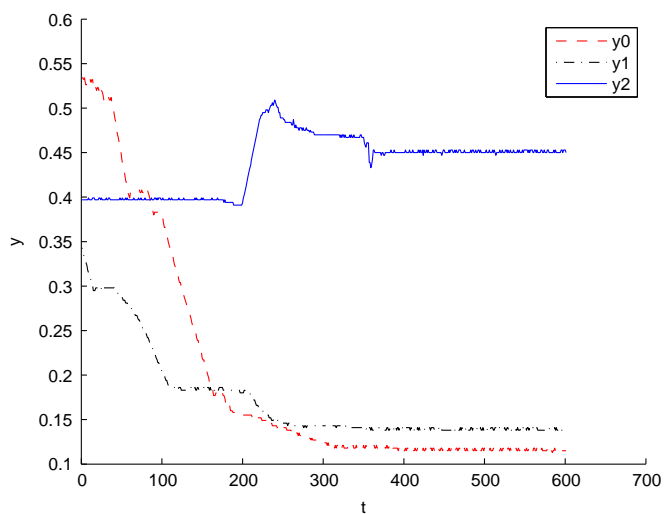


Fig. 16. The y coordinate of E-puck robots' position trajectory.

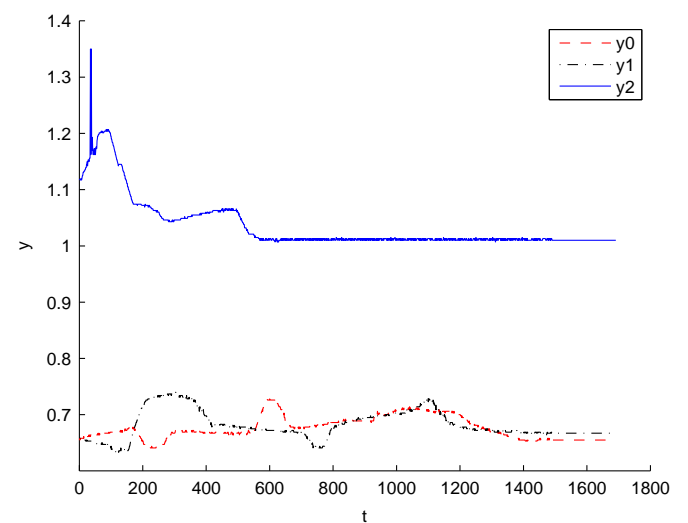


Fig. 18. The Y coordinate of E-puck robots with collision avoidance.

7. Conclusion

An optimal formation control strategy has been proposed using the estimated position information other than the absolute position of the second-order modeled agents in this paper. During the formation process the energy cost of each agent is minimized by solving the algebraic equation. The strategy is proved to be an effective solution to formation control by simulation. Then, a consensus law based on the estimator is presented, which enables the agents converge to the formation in a cooperative manner. The stability can be guaranteed by proper parameters. Moreover, an extra control input is added to the formation control, which can realize obstacle avoidance provided that the agents have the ability of detecting the environment around and the relative position p_{ij} . At last, we carry out real experiments using our formation strategy with E-puck robots and the results can verify the effectiveness of the algorithm.

There are some problems to be considered in future work. First problem is the formation control with variational desired trajectory other than desired points. Since in more realistic situation, the desired formation configurations are changing all time, and how to track the variational trajectory is what we should consider in the future. Second problem is how to propose the velocity estimator if the agents cannot get the absolute velocity of themselves by what means less energy cost. Finally, how to use the strategy to more complex realistic dynamic model is still an aspect to consider.

Acknowledgment

The authors would like to thank the referees for their valuable and helpful comments which have improved the presentation. The work was supported by the National Basic Research Program of China (973 Program) (2012CB720000), the National Natural Science Foundation of China (61225015), Foundation for Innovative Research Groups of the National Natural Science Foundation of China (Grant no. 61321002).

References

- [1] Olfati-Saber R, Fax JA, Murray RM. Consensus and cooperation in networked multi-agent systems. *Proc IEEE*, 2007;95(4):215–33.

- [2] Chen J, Xia Y. Formation control and obstacles avoidance for multi-agent systems based on position estimation. In: 2014 33rd Chinese control conference (CCC), IEEE, Nanjing, China; 2014. p. 1150–55.
- [3] Tsitsiklis J, Bertsekas D, Athans M. Distributed asynchronous deterministic and stochastic gradient optimization algorithms. *IEEE Trans Autom Control* 1986;31(9):803–12.
- [4] Ren W, Beard RW, Atkins EM. A survey of consensus problems in multi-agent coordination. In: Proceedings of the 2005 American control conference; 2005. p. 1859–64.
- [5] Abdessameud A, Tayebi A. On consensus algorithms design for double integrator dynamics. *Automatica* 2013;49(1):253–60.
- [6] He W, Cao J. Consensus control for high-order multi-agent systems. *Control Theory Appl*, IET 2011;5(1):231–8.
- [7] Naranjani Y, Sardahi Y, Chen YQ, Sun JQ. Multi-objective optimization of distributed-order fractional damping. *Commun Nonlinear Sci Numer Simul* 2015;24(1):159–68.
- [8] Chen H, Zhang J, Chen B, Li B. Global practical stabilization for non-holonomic mobile robots with uncalibrated visual parameters by using a switching controller. *IMA J Math Control Inf* 2013 dns044.
- [9] Chen H. Robust stabilization for a class of dynamic feedback uncertain non-holonomic mobile robots with input saturation. *Int J Control Autom Syst* 2014;12(6):1216–24.
- [11] Cui R, Ge SS, Ho BV, Choo Y. Leader follower formation control of under actuated autonomous under water vehicles. *Ocean Eng* 2010;37(17):1491–502.
- [12] Schoerling D, Kleck CV, Fahimi F, Koch CR, Ams A, Lober P. Experimental test of a robust formation controller for marine unmanned surface vessels. *Auton Robots* 2010;28(2):213–30.
- [13] Borhaug E, Pavlov A, Panteley E, Pettersen KY. Straight line path following for formations of underactuated marine surface vessels. *IEEE Trans Control Syst Technol* 2011;19(3):493–506.
- [14] Egerstedt M, Hu X, Stotsdy A. Control of mobile platforms using a virtual vehicle approach. *IEEE Trans Autom Control* 2011;46(11):1777–82.
- [15] Beard RW, Lawton J, Hadaegh FY. A coordination architecture for spacecraft formation control. *IEEE Trans Control Syst Technol* 2001;9(6):777–90.
- [16] Lawton JR, Beard RW. Synchronized multiple spacecraft rotations. *Automatica* 2002;38(8):1359–782.
- [17] Balch T, Arkin RC. Behavior-based formation control for multirobot teams. *IEEE Trans Robot Autom* 1998;14(6):926–39.
- [18] Koditschek DE, Rimon E. Robot navigation functions on manifolds with boundary. *Adv Appl Math* 1990;11(4):412–42.
- [19] Dimarogonas D, Kyriakopoulos K. Connectedness preserving distributed swarm aggregation for multiple kinematic robots. *IEEE Trans Robot* 2008;24(5):1213–23.
- [20] Zavlanos M, Tanner H, Jadbabaie A, Pappas G. Hybrid control for connectivity preserving flocking. *IEEE Trans Autom Control* 2009;54(12):2869–75.
- [21] Ren W, Beard RW, McLain TW. Coordination variables and consensus building in multiple vehicle systems. In: Cooperative control, Lecture notes in control and information sciences (LNCIS); 2004. p. 171–88.
- [22] Ren W, Beard RW. Distributed consensus in multi-vehicle cooperative control: theory and applications [M]. London: Springer-Verlag; 2008.
- [24] Oh K-K. Formation control of mobile agents based on distributed position estimation. *Autom Control* 2013;58(3):737–42.